JOURNAL OF CHEMICAL EDUCATION

LABORATORY EXPERIMENT

pubs.acs.org/jchemeduc

An Inversion Recovery NMR Kinetics Experiment

Travis J. Williams,* Allan D. Kershaw, Vincent Li, and Xinping Wu

Loker Hydrocarbon Research Institute and Department of Chemistry, University of Southern California, Los Angeles, California 90089-1661, United States

Supporting Information

ABSTRACT: A convenient laboratory experiment is described in which NMR magnetization transfer by inversion recovery is used to measure the kinetics and thermochemistry of amide bond rotation. The experiment utilizes Varian spectrometers with the VNMRJ 2.3 software, but can be easily adapted to any NMR platform. The procedures and sample data sets in this article will enable instructors to use inversion recovery as a laboratory activity in applied NMR classes and provide research students with a convenient template with which to acquire inversion recovery data on research samples.

KEYWORDS: Graduate Education/Research, Upper-Division Undergraduate, Analytical Chemistry, Laboratory Instruction, Hands-On Learning/Manipulatives, Computer-Based Learning, Equilibrium, Instrumental Methods, Kinetics, NMR Spectroscopy

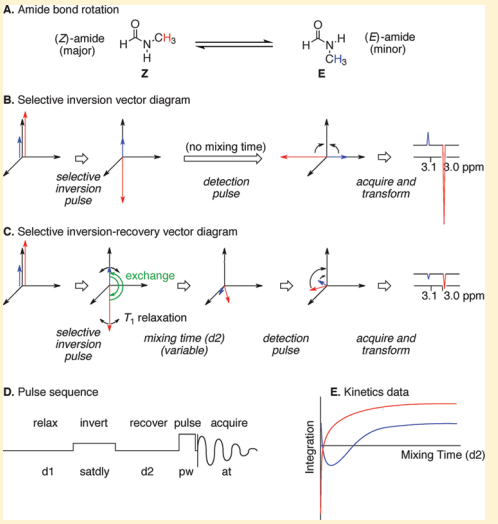

Nuclear magnetic resonance spectroscopy (NMR) is usually the first choice in structure determination for most organic molecules and organometallic complexes in the modern synthetic chemistry research laboratory. The importance of NMR techniques makes them important features of the curricula of the majority of chemistry doctoral programs, as well as many top undergraduate programs. Several excellent texts are available for NMR courses at both graduate[1] and undergraduate levels.[2] Many of these textbooks describe useful laboratory exercises relevant to synthetic organic chemistry. We found, however, that some techniques, particularly those that do not lend themselves to automated acquisition, are under-utilized in our NMR facility. To address this problem, we have developed an applied two-credit (half-time) laboratory course that covers practical NMR problems ranging in nature from structure determination to magnetization transfer kinetics studies. The students are required individually to collect and process data, then present their results in the *Journal of the American Chemical Society* communication format. We offer this course as the laboratory complement of a theoretically rigorous four-credit course on the principles of NMR. Each is available to both our graduate students and research-active undergraduate students.

Here we describe a lab exercise from our applied NMR course in which we use inversion recovery kinetics to measure the rotational barrier of *N*-methylformamide using Varian's VNMRJ 2.3 software.[3] Although this is the final and most technically challenging experiment in our NMR lab course, we find that it is well within the capability of first-year graduate students and advanced undergraduates that are properly instructed. This article and its accompanying Supporting Information should avail most instructors that have access to NMR processing software of all of the files needed to work through all of the data processing and analysis aspects of the experiment. In departments that have access to Varian spectrometers, this article should provide adequate instruction to replicate the experiment in their NMR laboratories.

THE MAGNETIZATION TRANSFER BY INVERSION RECOVERY NMR EXPERIMENT

Magnetization transfer has proven to be a powerful tool in studying slow chemical exchange processes. In general, magnetization transfer is an NMR experiment in which one proton signal in an equilibrium mixture is selectively "labeled" by spin saturation or inversion. While this spin relaxes during a mixing time, a chemical exchange process converts the labeled spin to a signal at different chemical shift. Acquiring spectra with different mixing times enables the extraction of both T_1 data (spin−lattice relaxation time constants) for all involved signals and the rate constant(s) for the chemical exchange. Because of the lower and upper rate boundaries, the T_1 and the minimum time for NMR acquisition, respectively, the rates most conveniently measured by inversion recovery are those with values around 10^{-1} s^{-1} and 10^{+1} s^{-1}.

Published: March 11, 2011

Scheme 1. Inversion Recovery NMR Kinetics Applied to Amide Bond Rotation

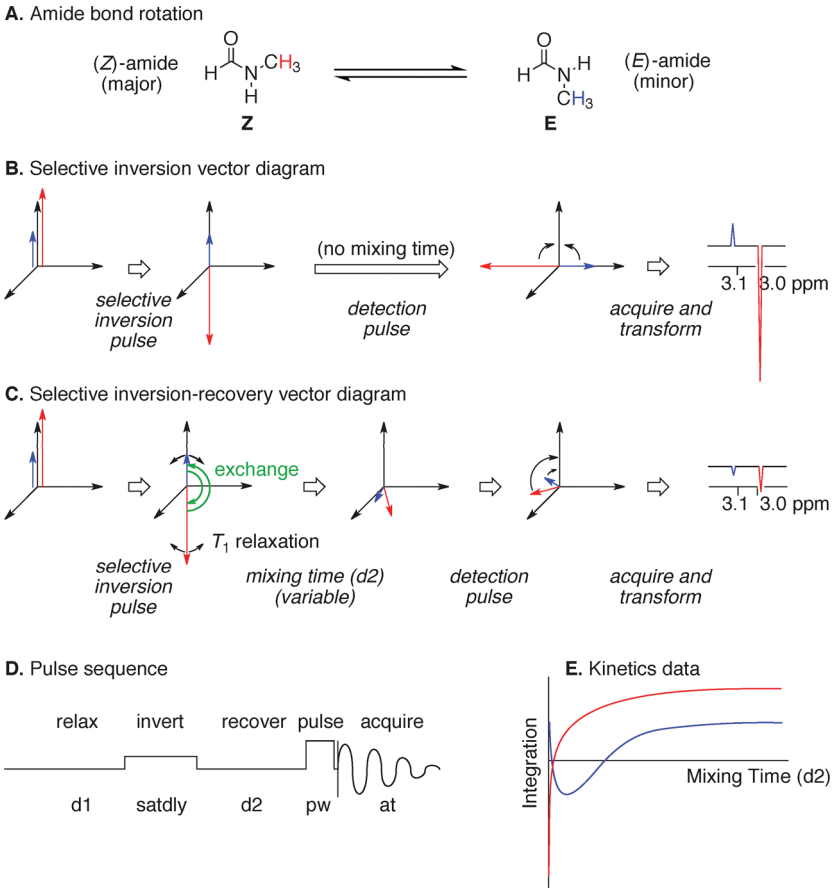

In 1958, McConnell presented modified Bloch equations in which chemical exchange was described.[4] Forsén and Hoffman suggested that if nucleus X is reversibly transferred between sites A and B in an exchanging system, then any disturbance in the nuclear spin of X should also be transferred by the chemical exchange, given that the spin−lattice relaxation time is large compared with the lifetime of the nucleus X in each site.[5] Thus, for magnetization transfer to work, we need $T_1^A \gg \tau_A$, where τ_A is the lifetime of magnetization in site A. In these circumstances, the McConnell−Bloch equations simplify to system of differential equations, which is shown in the Supporting Information. Although this system can be analytically solved, the solution cannot be expressed easily in terms of the exchange rate constant.

The magnetization transfer experiment requires selective excitation at a single frequency without disturbance of the neighboring signals, which is difficult to achieve. In 1976, Bodenhausen, Freeman, and Morris designed the pulse sequence "DANTE" specifically for selective excitation applied to the study of chemical exchange reactions.[6] Since then, 1D and 2D inversion recovery experiments have been widely used to study slow exchange chemical reactions.[7] However, 1D experiments have inherent advantages over the 2D experiments because the former can be easily quantified by 1D integration if desired. Extracting rate constants from data sets acquired in this way remained a specialty skill until Bain and Cramer introduced the freeware CIFIT program,[8] which simplifies the calculations required for modeling inversion recovery kinetic data to the extent that it can be easily achieved by skilled undergraduates. A current version of the CIFIT program is available from the Bain group Web page.[9]

Our implementation of the inversion recovery experiment is explained in Scheme 1. Line A illustrates the chemical exchange reaction for which a rate constant is measured. The ground state of *N*-methylformamide is (*Z*)-amide, **Z**.[10] This converts to amide **E** by rotation about the amide bond with a rate on the order of 1 s^{-1} at about 90 °C. Line B in Scheme 1 shows a rotating frame vector diagram for a selective inversion pulse sequence with no mixing time (inversion with no recovery). The spins start at rest, aligned along the $+Z$ axis. In this rendering, the red spin (**Z**) is shown to be longer than the blue spin (**E**) to indicate that it is the major isomer.[11] The first pulse of the sequence (Scheme 1D) is a single frequency, low power, 180° pulse on resonance with the red nucleus. This inverts the red proton (**Z**'s methyl group) relative to the blue proton (**E**'s methyl group). If there is no mixing time (d2 = 0), a second, hard, broadband pulse rotates all spins 90°, thus, preparing for acquisition. If there is a mixing time (d2 > 0) between the soft inversion pulse and the hard 90° pulse, then during this mixing time two processes take place. First, there is the chemical exchange, which swaps "negative" magnetization from the red peak with "positive" magnetization in the blue peak. This is a first-order exponential process that corresponds to the physical rotation of the amide bond interconverting the red and blue (*Z* and *E*) methyl groups. The second process is that both signals are undergoing spin−lattice relaxation back to the *z* axis.

If this experiment is repeated with various values of d2, a kinetics curve can be plotted as shown in Scheme 1E. The *x* axis of this graph is the mixing time d2, which is the time through which the two signals exchange before data are acquired. The *y* axis is the integration of the respective signals. In this particular rendering, one can see that the red

dx.doi.org/10.1021/ed1006822 |*J. Chem. Educ.* 2011, 88, 665–669

(**Z**) curve starts out negative, then grows quickly at first (fast exchange) and slowly later (T_1 relaxation). The blue curve illustrates the integration of the (*E*)-isomer as a function of mixing time (d2). It starts out positive, but dives downward as it exchanges magnetization with the (*Z*)-isomer via bond rotation. Eventually, it becomes positive again due to spin−lattice relaxation. Simultaneously, the rate constant for the exchange process and the T_1 values for (*Z*)- and (*E*)-protons can be determined by fitting these curves.

Once recorded, the kinetic magnetization data can be fitted into a two-site exchange model[4] using CIFIT.[10] Resulting values for magnetization and chemical exchange rates are given by CIFIT. These rate constants can be used to construct an Eyring plot for the bond rotation process. A van't Hoff plot can be prepared conveniently by measuring the equilibrium integrations of **E** and **Z**.

■ ACQUIRING THE DATA

In our hands, the pulse sequence diagrammed in Scheme 1D is most conveniently implemented on the Varian VNMRJ 2.3 software by adapting the sequence Presat in the Varian sequence library. A detailed procedure for this is summarized here. The Supporting Information contains notes, graphs, and crude data used in executing this experiment.

First, equilibrate the spectrometer to the desired temperature and acquire a Presat spectrum of *N*-methylformamide in water-d_2 with the saturation frequency set to the large singlet at about 3 ppm. This singlet corresponds to the red (**Z**) methyl group in Scheme 1A. Once this is acquired, the frequency for selective inversion (satfrq), the width of the inversion pulse (satpwr), and the spectral window (width, sw, and center, tof) are set. We find that a pulse sequence (acquisition time plus recycle delay, at +d1) of greater than 10 s is adequate to relax protons in *N*-methylformamide sufficiently for kinetics analysis. Some experimentation might be required for setting an appropriate d1, which might vary depending on the instrument, temperature, and sample.

Next, calibrate the width of the soft 180° pulse. To do so, array the value of the pulse width (satdly) starting with a minimum value slightly above the high power 90° pulse. Note that the default value of satdly is far larger than the one that will be used for inversion recovery. Figure 1 illustrates a plot of arrayed spectra in which an optimal 180° pulse width of satdly = 0.04 s is observed.

Before acquiring the kinetics run, it is necessary to set appropriate values of the interpulse delay, d2, into an array. Recall that d2 is going to be the time axis in our kinetics plot: we used 30−50 time points in our experiments. CIFIT will determine 7 parameters in the empirical fit, and 4 data points per parameter (28 total values of d2) is a suitable minimum. We observe that it is useful to acquire data through ca. 5 T_1 periods. We also observe that best results are obtained when the density of d2 values is higher near the beginning of the experiment, but we've experienced problems fitting data sets with too many points at small d2 times and too few at longer times.

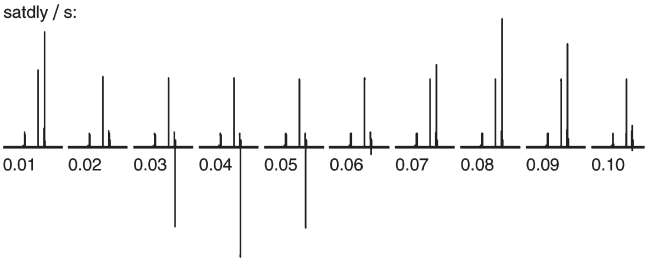

Figure 1. Example of stacked spectra for calibrating a 180° pulse. Data were acquired at 60.30 °C at 500 MHz. Optimal pulsewidth from this data set is satdly = 0.04 s.

■ HAZARDS

N-methylformamide may cause eye, skin, and respiratory tract irritation. It may be harmful if swallowed, inhaled, or absorbed through the skin.

■ FITTING DATA

The data sets included with this article can be easily fit with CIFIT according to the CIFIT instructions by using the initial guesses listed in the Supporting Information and the included CIFIT data and mechanism files. The mathematics behind CIFIT is explained in the CIFIT instruction manual: generally, the program takes initial guesses of rate and equilibrium parameters from a user-defined mechanism file. It conducts a least-squares minimization on the difference between the integration versus time curves in the user's data file and the curves predicted by the McConnell−Bloch equations given the initial guesses in the mechanism file.

We had no problems installing or using CIFIT, but we did observe that a number of student data sets did not converge in the CIFIT optimization. When it occurred, we determined that this problem was due to uneven distribution of d2 data points, usually too many data points at small d2 values. The measured rate constants reported in the CIFIT output files are summarized in Table 1. Note that the data shown in Table 1 were collected and submitted as homework responses by students in our NMR course with little or no supervision beyond classroom instruction. Thus, these represent first-pass results from new inversion recovery users.

Table 1. Measured Rate and Equilibrium Constants

Temperature/°C[a]	K/s^{-1}[b]	K_{eq}[c]
60	$4.0(12) \times 10^{-2}$	1.22×10^{-1}
65	$8.1(14) \times 10^{-2}$	1.28×10^{-1}
75	$2.3(3) \times 10^{-1}$	1.37×10^{-1}
82	$3.6(6) \times 10^{-1}$	1.43×10^{-1}
89	$9.9(36) \times 10^{-1}$	1.46×10^{-1}
103	$2.4(5) \times 10^{0}$	1.60×10^{-1}

[a] Temperatures were calibrated against an ethylene gycol standard provided by Varian. [b] Rate constants and their standard errors were generated by CIFIT. [c] Equilibrium constants were determined from ^{1}H integrations of *N*-methyl group in steady state proton spectra. Standard error on each value is shown in parentheses in terms of the last digit of the value.

■ CALCULATING THERMOCHEMICAL PARAMETERS

The activation parameters ($\Delta H^{\ddagger}$ and $\Delta S^{\ddagger}$) are obtained from an Eyring plot constructed from the measured rate constants (Figure 2).[12] These are determined from a plot of $R \ln(k/T) - 47.18$ cal/(mol K) versus $1000/T$. The plot will have slope of $-\Delta H^{\ddagger}$ in kcal mol^{-1} and *y* intercept of $\Delta S^{\ddagger}$ in cal mol^{-1} K^{-1}. This relationship is derived from the Eyring equation as illustrated in eqs 1−3. The factor of 1000 in the enthalpic term is incorporated to convert the units of $\Delta H^{\ddagger}$ from cal mol^{-1} to kcal mol^{-1}.

$$k = \frac{k_B T}{h} \times e^{-\Delta H^{\ddagger}/RT} \times e^{\Delta S^{\ddagger}/R} \quad (1)$$

dx.doi.org/10.1021/ed1006822 |J. Chem. Educ. 2011, 88, 665–669

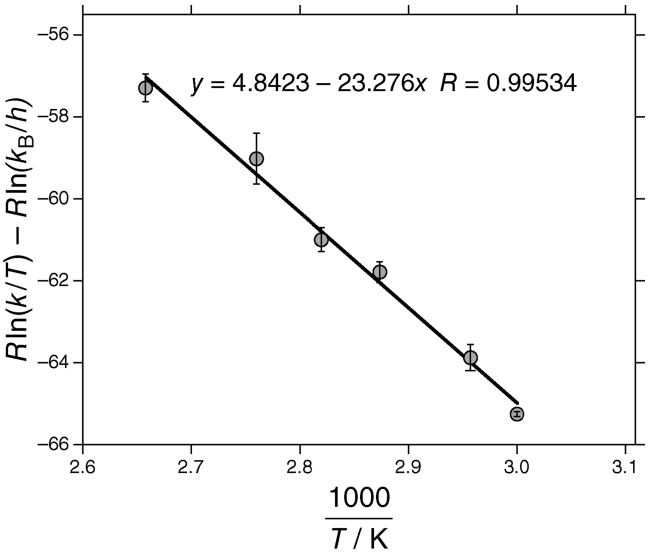

Figure 2. Eyring plot: $\Delta H^{\ddagger} = 23.2(7)$ kcal mol^{-1} and $\Delta S^{\ddagger} = 4.8(42)$ cal mol^{-1} K^{-1}.

$$R \ln\left(\frac{k}{T}\right) + R \ln\left(\frac{h}{k_B}\right) = -\Delta H^{\ddagger}\left(\frac{1}{T}\right) + \Delta S^{\ddagger} \quad (2)$$

$$R \ln\left(\frac{k}{T}\right) - 47.18 \text{ cal/(mol K)} = -\Delta H^{\ddagger}\left(\frac{1000}{T}\right) + \Delta S^{\ddagger} \quad (3)$$

where $R = 1.99$ cal mol^{-1} K^{-1}, $h = 6.63 \times 10^{-34}$ J s, and $k_B = 1.23 \times 10^{-23}$ J K^{-1}.

Standard error values for the activation parameters, $\sigma(\Delta H^{\ddagger})$ and $\sigma(\Delta S^{\ddagger})$, are available according to eqs 4 and 5, as derived by Girolami.[13] Notice that in both cases, the error decreases if data are collected over a broader temperature rage, ΔT. This is particularly important for $\Delta S^{\ddagger}$; in fact many experimentalists regard entropies of activation measured in this way as unreliable unless they are computed from a data set spanning greater than 40 °C.

$$(\sigma(\Delta H^{\ddagger}))^2 = \left(\frac{RT_{max}T_{min}}{\Delta T}\right)^2 \left\{ \left(\frac{\sigma(T)}{T}\right)^2 \left[\left(1 + T_{min}\frac{\Delta L}{\Delta T}\right)^2 + \left(1 + T_{max}\frac{\Delta L}{\Delta T}\right)^2 \right] + 2\left(\frac{\sigma(k)}{k}\right)^2 \right\} \quad (4)$$

$$(\sigma(\Delta S^{\ddagger}))^2 = \left(\frac{R}{\Delta T}\right)^2 \left\{ \left(\frac{\sigma(T)}{T}\right)^2 \left[T_{max}^2 \left(1 + T_{min}\frac{\Delta L}{\Delta T}\right)^2 + T_{min}^2 \left(1 + T_{max}\frac{\Delta L}{\Delta T}\right)^2 \right] + \left(\frac{\sigma(k)}{k}\right)^2 (T_{max}^2 + T_{min}^2) \right\} \quad (5)$$

with $\Delta T = T_{max} - T_{min}$; $\Delta L = \ln(k_{max}/T_{max}) - \ln(k_{min}/T_{min})$.

The equilibrium parameters (ΔH and ΔS) are obtained from a van't Hoff plot constructed from the measured equilibrium

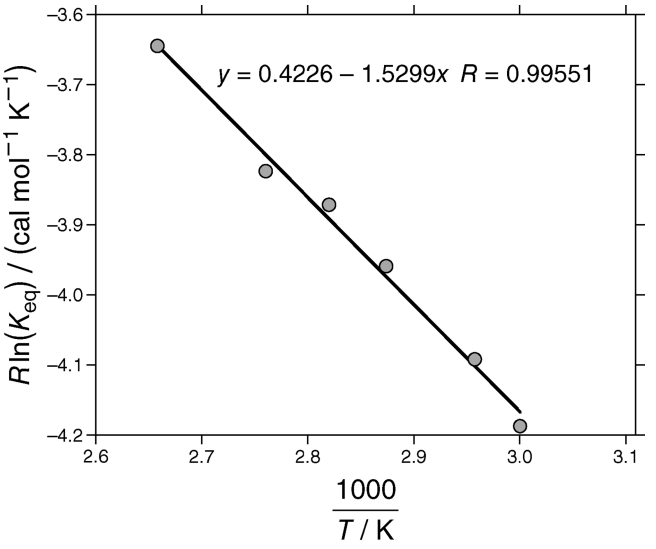

Figure 3. van't Hoff plot: $\Delta H = 1.53(7)$ kcal mol^{-1} and $\Delta S = 0.4(2)$ c.

constants (Figure 3). These are determined from a plot of $R \ln(K_{eq})$ versus $1000/T$. The plot will have slope of $-\Delta H$ (kcal mol^{-1}) and y intercept of ΔS (cal mol^{-1} K^{-1}). This relationship is derived from the van't Hoff equation as illustrated in eqs 6−8.

$$K_{eq} \equiv \frac{[E]}{[Z]} \quad (6)$$

$$\Delta G = -RT \ln(K_{eq}) = \Delta H - T\Delta S \quad (7)$$

$$R \ln(K_{eq}) = -\Delta H^{\ddagger}\left(\frac{1000}{T}\right) + \Delta S^{\ddagger} \quad (8)$$

Standard error values for the equilibrium parameters, $\sigma(\Delta H)$ and $\sigma(\Delta S)$, can be copied directly from the standard error calculation built in to any linear fit engine, such as Microsoft Excel (see the Supporting Information). Beware that calculating error in this way assumes that the error caused by deviation from linearity in the plot is larger than error resulting from uncertainties in the values of K_{eq}.

CONCLUSION

The procedures and data in this manuscript should enable instructors to use inversion recovery kinetics in advanced NMR laboratory courses and aid students in acquiring and processing inversion recovery data in their research. Furthermore, use of the provided NMR FID files with any Varian-compatible NMR processing software could be the basis of a very nice analytical problem set that demonstrates for students the process of determining energetic parameters from raw kinetics data. Ongoing educational research in our NMR facility includes the development of useful exercises to teach younger undergraduates both structure determination and basic analytical chemistry.

ASSOCIATED CONTENT

Supporting Information

Detailed procedures, notes, graphs, and simplified McConnell−Bloch equations; Varian FID files for all kinetics runs; CIFIT data,

mechanism, output files; and instructions to students. This material is available via the Internet at http://pubs.acs.org.

AUTHOR INFORMATION

Corresponding Author
*E-mail: travisw@usc.edu.

ACKNOWLEDGMENT

We are grateful to the National Science Foundation (DBI-0821671, CHE-0840366), the National Institutes of Health (1 S10 RR25432), and the University of Southern California for their sponsorship of NMR spectrometers at USC. We thank the ACS Petroleum Research Fund and the Hydrocarbon Research Foundation for research sponsorship and G. K. S. Prakash for valuable discussions. T.J.W. is grateful to the graduate students in the first offering of this course: A. Aviles, G. Belanger-Chabot, L. Gurung, A. Joyce, E. McAnally, D. Mustafa, M. Norako, M. Pirogovsky, S. Rodney, Y. Song, M. Williams, B. Zaro, and Z. Zhang.

REFERENCES

(1) (a) Claridge, T. D. W. *High-Resolution NMR Techniques in Organic Chemistry*, 2nd ed.; Elsevier: San Francisco, 2009. (b) Freeman, R. *Magentic Resonance in Chemistry and Medicine*; Oxford UP: Oxford, 2003. (c) Martin, G. E.; Zektzer, A. S. *Two-Dimensional NMR Methods for Establishing Molecular Connectivity*; VCH: New York, 1988.

(2) (a) Günther, H. *NMR Spectroscopy*, 2nd ed; John Wiley and Sons: New York, 1995. (b) Crews, P.; Rodríguez, J.; Jaspars, M. *Organic Structure Analysis*; Oxford UP: New York, 1998. (c) Pavia, D. L.; Lampman, G. M.; Kriz, G. S.; Vyvyan, J. A. *Introduction to Spectroscopy*, 4th ed. Brooks Cole: New York, 2008. (d) Rovnyak, D.; Stockland, R., Eds.; *Modern NMR Spectroscopy in Education; ACS Symposium Series 969*; American Chemical Society: Washington, DC, 2007.

(3) Our group developed this procedure for the following research project: Conley, B. L.; Williams, T. J. *J. Am. Chem. Soc.* **2010**, *132*, 1764–1765.

(4) McConnell, H. M. *J. Chem. Phys.* **1958**, *28*, 430–431.

(5) Forsén, S.; Hoffman, R. A. *J. Chem. Phys.* **1963**, *39*, 2892–2901.

(6) (a) Bodenhausen, G.; Freeman, R.; Morris, G. A. *J. Magn. Reson.* **1976**, *23*, 171–175. (b) Morris, G. A.; Freeman, R. *J. Magn. Reson.* **1978**, *29*, 433–462.

(7) (a) Mariappan, S. V. S.; Rabenstein, D. L. *J. Magn. Reson.* **1992**, *100*, 183–188. (b) Robinson, G.; Kuchel, P. W.; Chapman, B. E. *J. Magn. Reson.* **1985**, *63*, 314–319.

(8) Bain, A. D.; Cramer, J. A. *J. Magn. Reson.* **1996**, *118 A*, 21–27.

(9) Current URL: http://www.chemistry.mcmaster.ca/bain/.

(10) Schnur, D. M.; Yuh, Y. H.; Dalton, D. R. *J. Org. Chem.* **1989**, *54*, 3779–3785.

(11) Instructors should take care using this representation with students so as not to cause confusion between quantum mechanical and ensemble effects: a rotating-frame vector diagram usually represents the magnetization of a single nucleus. In this representation, the length of the arrows is used to represent the relative magnitude of magnetization in the experimental sample as a whole.

(12) For a discussion of Eyring plots, see Laidler, K. J.; King, M. C. *J. Phys. Chem.* **1983**, *13*, 1646–1655.

(13) Morse, P. M.; Spencer, M. D.; Wilson, S. R.; Girolami, G. S. *Organometallics* **1994**, *13*, 1646–1655.